arXiv:1704.01207v2 [stat.AP] 25 Jun 2017

Bayesian Model Averaging for the X-Chromosome Inactivation Dilemma in Genetic Association Study

Bo Chen, Radu V. Craiu* and Lei Sun*

Department of Statistical Sciences
University of Toronto
Toronto, ON M5S3G3, Canada
e-mail: craiu@utstat.toronto.edu
e-mail: sun@utstat.toronto.edu

Abstract: X-chromosome is often excluded from the so called 'whole-genome' association studies due to its intrinsic difference between males and females. One particular analytical challenge is the unknown status of X-inactivation, where one of the two X-chromosome variants in females may be randomly selected to be silenced. In the absence of biological evidence in favour of one specific model, we consider a Bayesian model averaging framework that offers a principled way to account for the inherent model uncertainty, providing model averaging-based posterior density intervals and Bayes factors. We examine the inferential properties of the proposed methods via extensive simulation studies, and we apply the methods to a genetic association study of an intestinal disease occurring in about twenty percent of Cystic Fibrosis patients. Compared with the results previously reported assuming the presence of inactivation, we show that the proposed Bayesian methods provide more feature-rich quantities that are useful in practice.

Keywords and phrases: Bayesian methods, Model uncertainty, Bayesian model averaging, Bayes factors, Markov chain Monte Carlo, Ranking, Genome-wide association studies.

1. Introduction

In the search for genetic markers that are responsible for heritable complex human traits, whole-genome scans including genome-wide association studies (GWAS) and the next generation sequencing (NGS) studies have made tremendous progress; see `www.genome.gov/gwastudies` for the most recent summary of GWAS findings by the National Human Genome Research Institute (Welter *et al.*, 2014). The 'whole-genome' nature of these studies, however, is often compromised by the omission of the X-chromosome (Heid *et al.*, 2010; Teslovich *et al.*, 2010). In fact, it was found that "*only 33% (242 out of 743 papers) reported including the X-chromosome in analyses*" based on the NHGRI GWAS Catalog (Wise *et al.*, 2013). The exclusion of X-chromosome from GWAS and NGS is due to it being fundamentally different between females and males. In contrast to the 22 autosomal chromosomes where both females and males have

*To whom correspondence should be addressed.

two copies, females have two copies of X-chromosome (XX) while males have only one X coupled with one Y-chromosome (XY). Thus, statistical association methods well developed for analyzing autosomes require additional considerations for valid and powerful application to X-chromosome.

Focusing on the single nucleotide polymorphisms (SNPs) as the genetic markers of interest here and without loss of generality, let d and D be the two alleles of a SNP and D be the risk allele. An X-chromosome SNP in females has three possible (unordered) genotypes, dd, dD and DD, in contrast to d and D in males. Suppose each copy of the D allele has an effect size of β on the outcome of interest; this β is the coefficient in linear regression for studying (approximately) normally distributed outcomes, or the log odds ratio in logistic regression for analyzing binary traits. To ensure "*dosage compensation for X-linked gene products between XX females and XY males*", X-chromosome inactivation (XCI) may occur so that one of the two alleles in females is randomly selected to be silenced (Gendrel & Heard, 2011). In other words, the effects of dd, dD and DD in females are now respectively 0, $\beta/2$ and β on average after XCI vs. 0, β and 2β without XCI. However, without collecting additional biological data the status of XCI is unknown.

Previous work on developing association methods for X-chromosome SNPs mostly focused on issues other than XCI, including the assumptions of Hardy-Weinberg equilibrium (HWE) and equal allele frequencies or sample sizes between female and males (Zheng *et al.*, 2007; Clayton, 2008). In his classic review paper, Clayton (2009) also discussed analytical strategies for multi-population or family-based studies. In each of these cases, either the XCI or no-XCI model is assumed, and naturally these methods work well only if the underlying assumption about the XCI status is correct (Loley *et al.*, 2011; Hickey & Bahlo, 2011; Konig *et al.*, 2014).

More recently, Wang *et al.* (2014) recognized the problem and proposed a maximum likelihood approach. In essence, the proposed method calculates multiple association statistics for testing the effect of a X-chromosome SNP under XCI and no XCI models, then uses the maximum. To adjust for the inherent selection bias, the method uses a permutation-based procedure to obtain the empirical distribution for the maximal test statistic and assess its significance. Although Wang *et al.*'s method appears to be adequate in terms of association testing, in the presence of model uncertainty it is not clear how to construct a point estimate or confidence interval for effect size β, or, what is a suitable measure of evidence for supporting one model over the other. Thus, an alternative paradigm that directly accounts for the inherent model uncertainty is desirable.

To close this gap, we propose a Bayesian approach that can handle in a principled manner the uncertainty about the XCI status. The use of Bayesian methods for genetic association studies is not new. Stephens & Balding (2009) and Craiu & Sun (2014) provide reviews in the context of studying autosome SNPs. Here we consider the posterior distributions generated from Bayesian regression models for analyzing X-chromosome SNPs under the XCI and no XCI assumptions. We combine the estimates from the two models following the Bayesian model averaging (BMA) principle that has long been recognized as

a proper method for incorporating model uncertainty in a Bayesian analysis (Draper, 1995; Hoeting *et al.*, 1999). We calculate the BMA-based highest posterior density (HPD) region for the parameter of interest. The BMA posterior distribution is directly interpretable as a weighted average for β, averaged over the XCI and no XCI models with more weight given to the one with stronger support from the data. To rank multiple SNPs, we calculate Bayes factors comparing the averaged model with the null model of no association for each SNP.

In Section 2, we present the theory of Bayesian model averaging for handling the X-chromosome inactivation uncertainty issue. We first consider linear regression models for studying continuous traits where closed-form solutions can be derived. We then discuss extension to logistic models for analyzing binary outcomes where Markov chain Monte Carlo (MCMC) methods are used for inference. In this setting, the calculation of Bayes factors is no longer possible analytically so we implement numerical approximations that have been reliably used in computing ratios of normalizing constants. To facilitate methods comparison, we also provide an analytical solution for assessing significance of the maximum statistic in the spirit of Wang *et al.* (2014), supplanting their permutation-based approach. In Section 3, we conduct extensive simulation studies to evaluate the performance of the proposed Bayesian approach. In Section 4, we apply the method to a X-chromosome association study of meconium ileus, an intestinal disease present in Cystic Fibrosis patients, providing further evidence of method performance. In Section 5, we discuss possible extensions and future work.

2. Methods

2.1. Normally distributed outcomes

The methodology development here focuses on linear models, studying association relationship between a (approximately) normally distributed trait/outcome Y and a X-chromosome SNP. Let (dd, dD, DD) and (d, D) be the genotypes of a SNP, respectively, for females and males. For autosome or X-chromosome SNPs in females, genotypes dd, dD and DD are typically coded additively as 0, 1 and 2, representing the number of copies of a reference allele, assumed to be D here. Under the X-chromosome inactivation (XCI) assumption, one of the two alleles of a female is randomly selected to have no effect on the outcome. Thus, the XCI and no XCI assumptions lead to two different coding schemes, respectively, G_1 and G_2 as summarized in Table 1.

Let Y be the vector of outcome measures of sample size n, and G_k be the vector of genotype values for the n individuals coded under model M_k, $k = 1$ and 2 as shown in Table 1. For each model M_k, we consider a linear regression model $Y = X_k\boldsymbol{\theta}_k + \epsilon_k$, where $X_k = (\mathbf{1}_n, G_k)$ is the design matrix, $\boldsymbol{\theta}_k = (\alpha_k, \beta_k)'$ and $\epsilon_k \sim N(0, \sigma^2 I_n)$. Here β_k represents the genetic effect of one copy of D under model $M_k, k = 1, 2$, accounting for the effects of other covariates Zs such as gender, age, smoking status and population information. For notation simplicity and without loss of generality for implementing the following Bayesian model

average framework, Zs are omitted from the regression model. The coding of 0.5 for genotype dD under M_1 reflects the fact that the effect of dD under the XCI assumption is the average of zero effect of d (if D was silenced) and β effect of D (if d was silenced). In addition, ϵ_1 and ϵ_2 have the same variance $\sigma^2 I_n$ because both models are based on same response variable Y.

Before we present the Bayesian approach, we make several important remarks here. First, the regression model above studies the genotype of a SNP, thus it does not require the assumption of HWE; only methods based on allele counts are sensitive to the equilibrium assumption (Sasieni, 1997). Similarly, allele-frequency affects only they efficiency of genotype-based association methods but not the accuracy. In addition, although other types of genetic architecture are possible, e.g. dD and DD having the same effect as in a dominant model or dd and dD having the same effect as in a recessive model, the additive assumption has its theoretical justification and sufficiently approximates many other models (Hill *et al.*, 2008).

2.2. A Bayesian model averaging approach

In practice, it is unknown which of the two models (M_1 XCI and M_2 no XCI) is true. Instead of performing inference based on only one of the two models or choosing the maximum one, the Bayesian model averaging (BMA) framework naturally aggregates information from both M_1 and M_2. Central to BMA is the Bayes factor (BF) defined as

$$BF_{12} = \frac{P(Y|M_1)}{P(Y|M_2)},$$

where $P(Y|M_k) = \int f(Y|\boldsymbol{\theta}, \sigma^2, M_k)\pi(\boldsymbol{\theta}|\sigma^2, M_k)\pi(\sigma^2|M_k)d\boldsymbol{\theta}d\sigma^2$ is the marginal probability of the data under model M_k. Here we used the outcome variable Y to denote all available data; meaning should be clear from the context.

We consider conjugate priors for $\pi(\sigma^2|M_k)$ and $\pi(\boldsymbol{\theta}|\sigma^2, M_k)$ for each model, $\pi(\sigma^2|M_k) = \pi(\sigma^2) = IG(a_0, b_0)$ where $IG(a_0, b_0)$ is the inverse gamma distribution with density function

$$p(\sigma^2) = \frac{b_0^{a_0}}{\Gamma(a_0)}(\sigma^2)^{-a_0-1}\exp\left(-\frac{b_0}{\sigma^2}\right).$$

As noted before, Y is common between M_1 and M_2 so the prior distributions of σ^2 for the two models are the same. For $\pi(\boldsymbol{\theta}|\sigma^2, M_k) = \pi(\boldsymbol{\theta}_k)$,

$$\pi(\boldsymbol{\theta}_k) = N(\boldsymbol{\mu_0}, \sigma^2\Lambda_{0k}^{-1}),$$

where Λ_{0k} is the precision matrix (Wright, 2008). For hyperparameter Λ_{0k}, we adopt the g-prior (Zellner, 1986) that takes the form of $\Lambda_{0k} = \frac{\lambda}{n}X_k'X_k$. We note that here the female component of G_1 is half of that of G_2. Thus, if we naïvely use $\pi(\boldsymbol{\theta}_k) = N(\boldsymbol{\mu_0}, \sigma^2\lambda I_2)$, this scaling factor can affect the Bayes factor and the ensuing model average quantities; the model with smaller covariate values

is always preferred even if rescaling is the only difference. We discuss further in Section 5 the importance of using the g-prior form in this setting.

When estimating the posterior distribution of $\boldsymbol{\theta}$ under each model, the effect of the precision parameter λ is minimal, but this is not true for inferring whether $\beta = 0$ or not using the Bayes factor. For the latter purpose, following the recommendations in Kass & Raftery (1995) we use $\lambda = 1$. For other hyperparameters, naturally $\boldsymbol{\mu_0} = \mathbf{0}$ unless there is prior information about association between the SNP under the study and the trait of interest. In the absence of additional information for σ^2, we let $a_0 = b_0 = 0.1$; setting $a_0 = b_0 = 0$ in simulation studies did not lead to noticeable numerical difference compared to $a_0 = b_0 = 0.1$.

The likelihood function is defined by $f(Y|\boldsymbol{\theta}, \sigma^2, M_k) \sim N(X_k\boldsymbol{\theta}, \sigma^2 I_n)$, which yields a normal-inverse-gamma posterior distribution, and the corresponding marginal distributions of $\boldsymbol{\theta}$ and σ^2 can be derived. Specifically, $\pi(\boldsymbol{\theta}, \sigma^2|Y, M_k)$, the posterior distributions for $(\boldsymbol{\theta}, \sigma^2)$ under each model M_k, is a multivariate t distribution with $2a$ degrees of freedom (df henceforth), location parameter $\boldsymbol{\mu_k}$ and scale parameter $\frac{b_k}{a}\Lambda_k^{-1}$, i.e., density function

$$\pi(\boldsymbol{\theta}|Y, M_k) \propto [1 + \frac{(\boldsymbol{\theta} - \boldsymbol{\mu}_k)'\Lambda_k(\boldsymbol{\theta} - \boldsymbol{\mu}_k)}{2b_k}]^{-\frac{2a+2}{2}},$$

and the posterior of σ^2 is $\pi(\sigma^2|Y, M_k) = IG(a, b_k)$, where

$$\Lambda_k = X_k'X_k + \Lambda_{0k} \quad (\Lambda_{0k} = \frac{\lambda}{n}X_k'X_k),$$

$$\boldsymbol{\mu}_k = \Lambda_k^{-1}(\Lambda_{0k}\boldsymbol{\mu_0} + X_k'Y),$$

$$a = a_0 + \frac{n}{2}, \text{ and } b_k = b_0 + \frac{1}{2}(Y'Y + \boldsymbol{\mu_0}'\Lambda_{0k}\boldsymbol{\mu_0} - \boldsymbol{\mu}_k'\Lambda_k\boldsymbol{\mu}_k).$$

Focusing on the primary parameter of interest here, we extract the slope coefficient β from the posterior of $\boldsymbol{\theta} = (\alpha, \beta)$ under each model M_k. If we let μ_{k2} be the second element of $\boldsymbol{\mu}_k$, and $(\Lambda_k^{-1})_{22}$ be the $(2,2)_{th}$ entry in Λ_k^{-1}, we obtain that β has univariate t distribution with $2a$ df and μ_{k2} and $\frac{b_k}{a}(\Lambda_k^{-1})_{22}$, respectively, as the location and scale parameters, i.e.

$$\pi(\beta|Y, M_k) = \mu_{k2} + t_{2a}\sqrt{\frac{b_k}{a}(\Lambda_k^{-1})_{22}}, \tag{2.1}$$

where t_{2a} is the standard t distribution with $2a$ df. The normalizing constant for the posterior under model M_k is then

$$P(Y|M_k) = \frac{f(Y|\boldsymbol{\theta}, \sigma^2, M_k)\pi(\boldsymbol{\theta}|\sigma^2, M_k)\pi(\sigma^2|M_k)}{\pi(\boldsymbol{\theta}, \sigma^2|Y, M_k)} = \frac{1}{(2\pi)^{n/2}}\sqrt{\frac{|\Lambda_{0k}|}{|\Lambda_k|}}\frac{b_0^{a_0}\Gamma(a)}{b_k^a\Gamma(a_0)},$$

which leads to the Bayes factor between M_1 and M_2 as

$$BF_{12} = \sqrt{\frac{|\Lambda_2|}{|\Lambda_1|} \times \frac{|\Lambda_{01}|}{|\Lambda_{02}|}}\left(\frac{b_2}{b_1}\right)^a. \tag{2.2}$$

The BMA of two models takes the form of (Hoeting *et al.*, 1999)

$$\pi(\boldsymbol{\theta}, \sigma^2|Y) \quad = \quad P(M_1|Y)\pi(\boldsymbol{\theta}, \sigma^2|Y, M_1) + P(M_2|Y)\pi(\boldsymbol{\theta}, \sigma^2|Y, M_2).$$

Let $P(Y)$ be the marginal probability of the data obtained after averaging over both models,

$$P(Y) = P(Y|M_1)P(M_1) + P(Y|M_2)P(M_2). \tag{2.3}$$

In the absence of prior information, it is customary to assume equal prior probabilities for the two models, i.e. $P(M_1) = P(M_2) = 0.5$. Therefore we have

$$\begin{aligned}\pi(\boldsymbol{\theta}, \sigma^2|Y) &= \frac{P(Y|M_1)P(M_1)}{P(Y|M_1)P(M_1) + P(Y|M_2)P(M_2)}\pi(\boldsymbol{\theta}, \sigma^2|Y, M_1) \\ &+ \frac{P(Y|M_2)P(M_2)}{P(Y|M_1)P(M_1) + P(Y|M_2)P(M_2)}\pi(\boldsymbol{\theta}, \sigma^2|Y, M_2) \\ &= \frac{BF_{12}}{1 + BF_{12}}\pi(\boldsymbol{\theta}, \sigma^2|Y, M_1) + \frac{1}{1 + BF_{12}}\pi(\boldsymbol{\theta}, \sigma^2|Y, M_2). \end{aligned} \tag{2.4}$$

Note that the posterior distribution $\pi(\boldsymbol{\theta}, \sigma^2|Y)$, which we call *BMA posterior*, is a mixture of the two posterior distributions resulting from models M_1 and M_2. Because it is not obtained from a given sampling distribution and a particular prior, it may not be a canonical posterior.

The BMA posterior relies on the Bayes factor as the weighting factor, favouring one model over using weights based on BF_{12}. Given an established association, we expect the Bayes factor provide evidence supporting one of the two models. Intuitively, if $BF_{12} > 1$ then we have more support for M_1 from the data and vice versa when $BF_{12} < 1$. For the priors considered here, we show in the Supplementary Materials that when data was generated from M_1, $Y = X_1\boldsymbol{\theta}_1 + \epsilon_1$, $BF_{12} \xrightarrow{p} \infty$ as $n \to \infty$ for any values of the hyperparameters, and similarly when $Y = X_2\boldsymbol{\theta}_2 + \epsilon_2$, $BF_{12} \xrightarrow{p} 0$. This is also consistent with our empirical observations from simulation studies, supporting the use of Bayes factor for model selection in this setting.

2.3. BMA-based highest posterior density interval for the genetic effect of a SNP

There are multiple ways to assess the genetic effect of a SNP based on the posterior distribution of β. The simpler approach is to use the posterior mode of β as a point estimate. The highest posterior density (HPD) region however provides more information with an interval estimate. To calculate BMA-based HPD, we note that the posterior density of β from each of the M_1 and M_2 models is a univariate t with location and scale parameters as specified in equation (2.1). The BMA posterior of β is therefore a mixture of two known t distributions with the mixture proportion depending on BF_{12}. It is thus possible to calculate the exact HPD region for β.

A $(1-\alpha)\%$ HPD is defined as $R(c_\alpha) = \{\beta : \pi(\beta|Y) \geq c_\alpha\}$, where $\pi(\beta|Y)$ is the BMA posterior density of β and c_α is the threshold such that the area under the posterior density is $1-\alpha$. Depending on the similarity between the two posterior distributions corresponding to M_1 and M_2 for a given credible level α, a BMA HPD region can be either one single interval or made up of two disconnected intervals. In all examples we have studied the HPD region is a single interval at $\alpha = 0.05$. Specifically, let β_l and β_u to be the two solutions of $\pi^{-1}(c_\alpha)$. The $1-\alpha$ HPD region is then (β_l, β_u), where

$$\int_{\beta_l}^{\beta_u} \pi(\beta|Y)d\beta = 1-\alpha,$$
$$\pi(\beta_l|Y) = \pi(\beta_u|Y) = c_\alpha. \tag{2.5}$$

The closed form of $\pi(\beta|Y)$ is in fact available, thus we can solve the equations defined in (2.5) numerically to find c_α as well as β_l and β_u, using function `multiroot` in R package `rootSolve`. Note that for notation simplicity, we use α here to denote the desired credible level; its distinction from the intercept parameter, also denoted by α, should be clear from the context.

2.4. Assessing genetic effect and ranking multiple SNPs by Bayes factor

In Bayesian framework, the significance of a SNP can be evaluated using Bayes factor (Kass & Raftery, 1995; Stephens & Balding, 2009). In the presence of model uncertainty, we propose using the Bayes factor calculated by comparing the averaging model between M_1 and M_2 with the null model of no effect, M_N. Under the null model of $\beta = 0$, let $X_N = \mathbf{1_n}$ be the corresponding design matrix. Using the same prior distributions and hyperparameter values for the remaining parameters, σ^2 and α, the calculation of $P(Y|M_N)$ is then similar to that of $P(Y|M_1)$ and $P(Y|M_2)$ as described in Section 2.2. Let

$$BF_{1N} = \frac{P(Y|M_1)}{P(Y|M_N)}, \quad BF_{2N} = \frac{P(Y|M_2)}{P(Y|M_N)}$$

be the Bayes factors comparing, respectively, the XCI M_1 and no XCI M_2 with the null model M_N, the Bayes factor for comparing the averaging model with the null model is defined as

$$BF_{AN} = \frac{P(Y|M_1)P(M_1) + P(Y|M_2)P(M_2)}{P(Y|M_N)}.$$

Because $P(M_1) = P(M_2) = 0.5$ in our setting, we thus have

$$BF_{AN} = \frac{1}{2}(BF_{1N} + BF_{2N}). \tag{2.6}$$

The Bayes factor BF_{AN} has similar asymptotic properties as BF_{12}. We show in the Supplementary Materials that in our setting if $\lambda > 0$ (the precision parameter

for β), then BF_{AN} converges in probability to either 0 or ∞, depending on whether $\beta = 0$ or not.

In practice, besides assessing association evidence for a single SNP, scientists are often interested in ranking multiple SNPs from a whole-genome scan and selecting the top ones for follow up studies. The (conservative) lower bounds of the HPD intervals (and the BFs) can be used for this purpose, and we demonstrate this in Section 4 where we rank over 14,000 X-chromosome SNPs studying their association evidence with meconium ileus in Cystic Fibrosis patients.

2.5. Binary outcomes

When we measure binary responses, M_1 and M_2 are logistic regression models. Assuming the prior $\boldsymbol{\theta}_k \sim N(\boldsymbol{\mu_0}, \Lambda_{0k}^{-1})$, the BMA framework described above can still be used although computational complexities arise due to the lack of conjugacy. Given its superior performance (Choi & Hobert, 2013), we use the Polya-Gamma sampler of Polson *et al.* (2013) and the R package `BayesLogit` to draw samples from the posterior distributions under M_1 and M_2. To obtain samples from the averaged model, we draw samples from M_1 with probability $BF_{12}/(1 + BF_{12})$ and from M_2 with probability $1/(1 + BF_{12})$ based on equation (2.4). And we use these samples to construct the $1 - \alpha$ HPD interval via the function `HPDinterval` in the R package `coda`.

The calculation of BF_{12} is based on the Bridge sampling method proposed by Meng & Wong (1996) and further refined by Gelman & Meng (1998) which we delineate below. Suppose we have J posterior samples, $\boldsymbol{\theta_{kj}}$, from the two models, $k = 1$ and 2 and $j = 1, ..., J$. For each parameter sample $\boldsymbol{\theta_{kj}}$, we can calculate the corresponding unnormalized posterior density based on the logistic model under the M_1 XCI assumption,

$$\begin{aligned} q_1(\boldsymbol{\theta_{kj}}) &= \pi(\boldsymbol{\theta_{kj}}|M_1) f(Y|\boldsymbol{\theta_{kj}}, M_1) \\ &= \pi_1(\boldsymbol{\theta_{kj}}) \prod_{i=1}^{n} p_{1i}(\boldsymbol{\theta_{kj}})^{Y_i} (1 - p_{1i}(\boldsymbol{\theta_{kj}}))^{1-Y_i}, \end{aligned}$$

where $p_{1i}(\boldsymbol{\theta_{kj}}) = [1 + \exp(-X_{1i}\boldsymbol{\theta_{kj}})]^{-1}$, and X_{1i} is the i_{th} row of the design matrix X_1 that contains the genotype data coded under model M_1 for the i_{th} individual. π_1 is the density function of $N(\boldsymbol{\mu_0}, \Lambda_{01}^{-1})$. Similarly we obtain

$$\begin{aligned} q_2(\boldsymbol{\theta_{kj}}) &= \pi(\boldsymbol{\theta_{kj}}|M_2) f(Y|\boldsymbol{\theta_{kj}}, M_2) \\ &= \pi_2(\boldsymbol{\theta_{kj}}) \prod_{i=1}^{n} p_{2i}(\boldsymbol{\theta_{kj}})^{Y_i} (1 - p_{2i}(\boldsymbol{\theta_{kj}}))^{1-Y_i}, \end{aligned}$$

where $p_{2i}(\boldsymbol{\theta_{kj}}) = [1 + \exp(-X_{2i}\boldsymbol{\theta_{kj}})]^{-1}$ under model M_2, and π_2 is the density function of $N(\boldsymbol{\mu_0}, \Lambda_{02}^{-1})$. We then define the ratio of unnormalized densities as $l_{kj} = q_1(\boldsymbol{\theta_{kj}})/q_2(\boldsymbol{\theta_{kj}})$ and compute the Bayes factor iteratively. Specifically, we

set $BF_{12}^{(1)} = 1$ and compute at the $(t+1)_{th}$ iteration until convergence,

$$BF_{12}^{(t+1)} = \frac{\sum_{j=1}^{J} \frac{l_{2j}}{l_{2j}+BF_{12}^{(t)}}}{\sum_{j=1}^{J} \frac{1}{l_{1j}+BF_{12}^{(t)}}}. \tag{2.7}$$

When comparing the averaged model vs. null model, the above procedure cannot be directly implemented to calculate BF_{1N} and BF_{2N}, since the null model has different dimension of parameter $\boldsymbol{\theta}$. Instead of finding the ratio of normalizing constants by the numerical method above, we find $P(Y|M_1)$, $P(Y|M_2)$ and $P(Y|M_N)$ by calculating the ratio between them and known quantities. The latter will be the normalizing constants corresponding to Gaussian approximations of the posterior distributions of interest. More precisely, we use the following steps:

- To calculate $P(Y|M_1)$, we approximate the posterior under M_1 using a bivariate normal distribution with independent components. So we find the sample mean and sample variance of posterior sample $\boldsymbol{\theta_{1j}} = (\alpha_{1j}, \beta_{1j})$, which are $(\bar{\alpha}_1, \bar{\beta}_1)$ and $\begin{pmatrix} s^2_{\alpha_1} & 0 \\ 0 & s^2_{\beta_1} \end{pmatrix}$.
- We simulate α'_{1j} and β'_{1j} from the above bivariate approximation to the posterior whose normalizing constant is $c_1 = 2\pi s_{\alpha_1} s_{\beta_1}$ and set $\boldsymbol{\theta'_{1j}} = (\alpha'_{1j}, \beta'_{1j})$.
- We use the iterative approach in equation (2.7) to compute the ratio of normalizing constants between the posterior under M_1 and the corresponding approximation, $BF_1 = P(Y|M_1)/c_1$. Since c_1 is known, we can easily derive the normalizing constant $P(Y|M_1)$.
- To calculate $P(Y|M_N)$, we repeat the procedure used for $P(Y|M_1)$ but this time the dimension of the parameter is one instead of two.
- The unnormalized posterior density for M_N is

$$\begin{aligned} q_N(\theta_{Nj}) &= \pi(\theta_{Nj}|M_N) f(Y|\theta_{Nj}, M_N) \\ &= \pi_N(\theta_{Nj}) \prod_{i=1}^{n} p_N(\theta_{Nj})^{Y_i} (1 - p_N(\theta_{Nj}))^{1-Y_i}, \end{aligned}$$

  where $p_N(\theta_{Nj}) = [1+\exp(-\theta_{Nj})]^{-1}$, and π_N is the prior density of $N(0, \lambda^{-1})$.
- We then use equation (2.7) to compute $BF_N = P(Y|M_N)/c_N$, and we obtain BF_{1N} as

$$BF_{1N} = \frac{BF_1}{BF_N} \times \frac{c_1}{c_N}.$$

- We repeat the above steps for M_2 to calculate BF_{2N}.
- Finally, we use equation (2.6) to calculate BF_{AN} by averaging BF_{1N} and BF_{2N}.

2.6. Revisit the maximum likelihood approach of Wang et al. (2014)

Let Z_1 and Z_2 be the frequentist's test statistics for testing $\beta_k = 0$ derived from the two regression models, $Y = \alpha_k + \beta_k G_k + \epsilon_k, k = 1$ and 2, respectively under

the XCI M_1 and no XCI M_2 assumptions; G_k are the corresponding genotype codings as shown in Table 1. The maximum likelihood approach of Wang *et al.* (2014), in essence, uses $Z_{max} = max(|Z_1|, |Z_2|)$ as the test statistic and calculates the p-value of Z_{max} empirically via a permutation-based procedure. Instead of obtaining p-values using a permutation-based method as discussed in Wang *et al.* (2014), we note that the significance of Z_{max} can be obtained more efficiently. Under the null hypothesis of no association for either linear or logistic regression, Z_1 and Z_2 have an approximate bivariate normal distribution, $N(\mathbf{0}, \Sigma)$ and $\Sigma = \begin{pmatrix} 1 & \rho_{Z_1,Z_2} \\ \rho_{Z_1,Z_2} & 1 \end{pmatrix}$, where conditional on the observed genotypes G_1 and G_2, $\rho_{Z_1|G_1,Z_2|G_2} = r_{G_1,G_2}$, where r_{G_1,G_2} is the sample correlation of G_1 and G_2. This principle has been used in another setting where for an un-genotyped SNP, instead of imputing the missing genotype data, the association statistic is directly inferred based on the association statistic at a genotyped SNP and the correlation between the two SNPs estimated from a reference sample (Lee *et al.*, 2013; Pasaniuc *et al.*, 2014). Thus, given the two genotype codings of each SNP, without permutation we can find the threshold value $z_{1-\alpha}$ for the maximum statistic Z_{max} at the nominal type I error rate of α. In application study below (Section 4), for each of the 14,000 or so SNPs analyzed, we will obtain the corresponding p-value using this method.

3. Simulation Study

We conduct simulation studies to evaluate the performance of the proposed Bayesian model averaging methods for studying both normally distributed traits and binary outcomes. Here we focus on the performance quantities relevant to Bayesian methods, including the BMA HPD internals of Section 2.3 and the BMA BF of Section 2.4. We leave the ranking comparison with the frequentist method of Wang *et al.* (2014) to the application study in Section 4.

3.1. Simulation settings

In our simulations, we vary the sample size n, proportion of males and frequencies of allele D for males and females (p_m and p_f respectively). In each case we first generate data for G, where we simulate female genotypes using a multinomial distribution with probabilities of $(1-p_f)^2$, $2p_f(1-p_f)$ and p_f^2, respectively, for dd, dD and DD, and we simulate male genotypes using a binomial distribution with probabilities of $(1-p_m)$ and p_m, respectively, for d and D.

We then generate outcome data for Y based on the simulated G coded under the XCI M_1 or no XCI M_2 assumption, and various parameter values of the regression models. For linear models we fix $\alpha = 0$; the intercept parameter has negligible effects on result interpretation (e.g. $\alpha = 1$ lead to similar conclusion). Without loss of generality, we also fix $\sigma^2 = 1$. Under the null model, $\beta = 0$ and Y does not depend on the XCI and no XCI assumptions, i.e. $Y \sim N(0, \sigma^2 I_n)$.

Under alternatives and for each M_k, method performance depends on both genetic effect size β and allele frequencies p_m and p_f, via the quantity EV, the variation of Y explained by genotype, where $EV = Var(E(Y|G))/Var(Y)$. Although allele frequencies affect method performance as we will see in the application study below, fixing EV instead of β has the benefit of not requiring specification of the relationship between β and allele frequencies (e.g. variants with lower frequencies tend to have bigger effects or smaller effects, vs. the two parameters are independent of each other); Derkach *et al.* (2014) explored this in a frequentist setting for jointly analyzing multiple autosome SNPs. For linear models, it is easy to show that $EV = \beta^2\sigma_G^2/(\beta^2\sigma_G^2 + \sigma^2)$, where σ_G^2 is the variance of G depending on p_m and p_f. Thus, for a given EV value we obtain $\beta = \sigma/\sigma_G \cdot \sqrt{EV/(1-EV)}$ for different choices of p_m and p_f and codings of G for M_k, $k = 1$ and 2. We then simulate Y for continuous outcomes from $N(X_k\boldsymbol{\theta}, \sigma^2 I_n)$ based on $\boldsymbol{\theta} = (\alpha, \beta)$ and $X_k = (\mathbf{1}_n, G_k)$.

For studying binary outcomes using logistic regression, we assume the typical study design of equal numbers of cases and controls. Under the null of $\beta = 0$, we randomly assign $Y = 0$ to half of the sample and $Y = 1$ to the other half. Under alternatives, the derivation of β given EV and allele frequencies is a bit more involved, and we outline the details in the Supplementary Materials. We then simulate Y from $Bin(n^*, (1 + \exp(-X_k\boldsymbol{\theta}))^{-1})$, $n^* > n$, until $n/2$ numbers of cases and controls are generated.

To summarize, the parameters involved in the simulation studies include the sample size (n and the proportion of males), allele frequencies in males and females (p_m and p_f), the variation of Y explained by genotype (EV and in turn β; without loss of generality (w.l.g.), $\alpha = 0$, $\sigma^2 = 1$), as well as equal numbers of cases and controls for studying binary traits. In the following, we show representative results when $n = 1000$ (and assuming the proportion of males is half), $EV = 0.005$ or 0.01, and p_m and p_f ranging from 0.1 to 0.9 where the two frequencies do not have to be equal but have to be both ≥ 0.5 or ≤ 0.5; in practice it is unlikely that the difference in allele frequencies is so big that the reference alleles in males and females differ. The number of MCMC samples for analyzing each binary dataset is $J = 1000$.

3.2. Performance of the Bayesian methods

We provide BMA-based HPD intervals and their corresponding BF_{AN} on the log_{10} scale for 50 independent data replicates simulated under different conditions for logistic regression models in Figures 1 and 2; results for linear models are provided in the Supplementary Materials. The intervals are sorted by their lower bounds. In the left-panel of each figure, the blue dashed line marks $\beta = 0$ and the red solid line marks the true value of β; two lines overlap under the null. In the right panel, the blue dashed line marks $log_{10}(BF_{AN}) = 0$, and the red solid line marks the conventional threshold of $log_{10}(BF_{AN}) = 1$ for declaring strong evidence favouring one model over the other (Kass & Raftery, 1995).

Figures 1 present the results under the null of no association where $EV = 0$

(i.e. $\beta = 0$). The top panel is for unequal male and female allele frequencies at (p_m, p_f)=(0.1, 0.3), and the bottom panel is for (p_m, p_f)=(0.3, 0.3); results for other allele frequency values (e.g. (0.5, 0.3), (0.5, 0.7), (0.7, 0.7) and (0.9, 0.7)) are similar and provided in the Supplementary Materials. We note that although the HPD intervals do not have the same coverage interpretation as CI, just over 95% of the HPD intervals contain zero. Similarly, most of the values are less than zero, i.e. $BF_{AN} < 1$; additional simulations show that BF_{AN} decrease as the sample size increases under the null.

Figures 2 presents the results under different alternatives, where (p_m, p_f)=(0.1, 0.3) and data are simulated from the XCI M_1 model, but EV varies and EV=0.005 for the top panel and EV=0.01 for the bottom; results for other parameter values and data simulated from M_2 are similar and are included in the Supplementary Materials. It is clear that as EV increases, the performance of the proposed Bayesian methods increases.

4. Application Study

Sun *et al.* (2012) performed a whole-genome association scan on meconium ileus, a binary intestinal disease occurring in about 20% of the individuals with Cystic Fibrosis. Their GWAS included X-chromosome but assumed the inactivation M_1 model. They identified a gene called *SLCA14* to be associated with meconium ileus, and in their Table 2 they reported p-values in the range of 10^{-12}, 10^{-8} and 10^{-6}, respectively, for $rs3788766$, $rs5905283$ and $rs12839137$ from the region. We revisit this data by applying the maximum likelihood approach (or the minimal p-value of the XCI M_1 and no XCI M_2 models) and the proposed Bayesian model average method.

The data consists of n = 3199 independent CF patients, and there are slightly more males (n_m = 1722, 53.8%) than females (n_f = 1477). Among the study subjects, 574 are cases with meconium ileus and 2625 are controls, and the rates of meconium ileus (17.7% vs. 18.3%) do not appear to differ between the male and female groups. Genotypes are available for 14280 X-chromosome SNPs, but 60 are monomorphic (no variation in the genotypes). Thus association analysis is performed between each of the 14220 X-chromosome SNPs and the binary outcome of interest. That is, 14220 p-values and 14220 BMA BFs and HPD intervals are calculated and investigated. By convention, for each SNP we assume the minor allele as the risk allele D and we use the two coding schemes as described in Table 1 under the M_1 and M_2 models.

Figure 3 shows the QQplots of p-values obtained using the frequentist framework. The left graph is under the M_1 inactivation assumption as in the original analysis of (Sun *et al.*, 2012). The middle one is under the M_2 no inactivation assumption. And the right one is based on the minimal p-values adjusted for selecting the best of the two models using the asymptotic approximation as discussed in Section 2.6. As expected, most of the SNPs are from the null, but there are four clear outliers/signals with evidence for association with meconium ileus regardless of the methods used. The overall consistency between the M_1 and M_2

models is the result of high correlation between Z_1 and Z_2; we discuss this point further in Section 5 below. Contrasting the left graph with the middle one in Figure 3 shows that the XCI M_1 assumption lead to smaller p-values for these four SNPs than the no XCI M_2 assumption. Table 2 provides the corresponding minor allele frequencies (MAF, pooled estimates because sex-specific estimates are very similar to each other), log OR estimates and p-values for these four SNPs.

Figure 4 present the Bayesian results for top 50 ranked SNPs. Similarly to the presentation of the simulation results in Section 3, in the left graph SNPs are ranked based on the lower bounds of their BMA-based HPD intervals, and the corresponding $log_{10}(BF_{AN})$ values are provided one the right. Table 3 provides more detailed results for top 15 SNPs including the BF_{12} comparing M_1 with M_2. Note that for ease of presentation and without loss of generality we mirror all negative intervals to positive ones.

Two important remarks can be made here. First, the proposed Bayesian method clearly identifies the four SNPs suggested by the p-value approach. Second, the Bayesian framework in this setting provides more feature-rich quantities, and it pinpoints additional SNPs that merit follow-up studies. Note that although p-values lead to similar rankings between the two models themselves, they could miss potentially important SNPs. Taking $rs12689325$ as an example, this SNP will not be identified with a rank of 331 based on the p-value of 0.0268, the adjusted minimum of p-values calculated under M_1 and M_2. However, this SNP ranks second based on the (conservative) lower bounds of the BMA-based HPD intervals averaged over M_1 and M_2 (Figure 4 and Table 3). The wide BMA HPD interval is a result of small MAF (1.3%) coupled with a moderate effect size. Given a trait of interest in practice, if genetic etiology implies the involvement of rare variants, the Bayesian results suggest that this SNP warrants additional investigation.

5. Discussion

We propose a Bayesian approach to address the ambiguity involved in GWAS and NGS studies of SNPs situated on the X-chromosome. Depending on whether X-inactivation takes place or not, there are two regression models that can be used to explore the genetic effect of a given SNP on the phenotype of interest. The proposed method allows us to produce posterior-based inference that incorporates the uncertainty within and between genetic models. While the former is quantified by the posterior distribution under each model, the latter can be properly accounted for by considering a weighted average of the model-specific estimators. Following the Bayesian paradigm, the weights are proportional to the Bayes factor comparing the two competing models. The asymptotic properties of the Bayes factors considered in this paper for linear models are included in the Supplementary Materials. In the binary response case, the theoretical study is difficult due to the intractable posteriors, but the Monte Carlo estimators exhibit good properties in all the numerical studies performed.

The use of g-priors in this study setting is essential in that it allows us to avoid the effect of covariate rescaling on the Bayes factors, yet maintain results interpretation. In regression models, we know that the effect size β is inversely proportional to the size of the covariate value/genotype coding. Given a set of data, using $X/2$ or X should lead to identical inference. However, without g-priors, a model with smaller covariate value would be preferred based on BF. In our setting, the female component of the design matrix under the XCI M_1 coding is only half of that no XCI M_2 coding; male codings are the same for the two models. Consider the null case of $\beta = 0$ when the two competing models are identical. Using $\Lambda_{0k} = \lambda I$ for the precision of $\boldsymbol{\theta_k}$, we see that 80% of BF_{12} are greater than one, suggesting M_1 is preferred simply because of its smaller genotype coding. One statistical solution is to rescale the design matrix prior to the Bayesian inference. However, it is important to note that the coding difference for females is driven by a specific biological consideration, thus rescaling leads to difficulties in results interpretation. Instead, we use a g-prior in Section 2. Indeed, simulation results for the null case show that $BF_{12} > 1$ in about 50% of replicates, indicating proper calibration.

The application has shown that the two models/assumptions lead to similar results, and one may argue that the practical benefits of using BMA-based inference is limited. However, It's important to note that while the wrong model may still lead to an average $log(BF)$ greater than one for a SNP, it significantly impacts the ranking of the SNP; in practice only a few top ranked SNPs receive the (often much more costly) biological experiments. Further, the similarity between the two models depends on the sample correlation between the covariates in the two models, r_{G_1,G_2}, which in turn depends on the allele frequency of the reference allele. In the Supplementary Materials, we derive the theoretical correlation, ρ_{G_1,G_2}, as a function of allele frequencies in males and females (p_m, p_f), and we show that when $\min\{p_m, p_f\}$ is not close to 1, G_1 and G_2 are indeed highly correlated. But when both p_m and p_f are large (e.g. $p_m = p_f = 0.95$), the correlation can be lower than 0.5. In that case, the two models will likely lead to different conclusions while the BMA-based approach remains robust. To illustrate, consider the linear model as before ($n = 1000$, $EV = 0.01$) but $p_m = p_f = 0.95$ and the true simulating model is either M_1 or M_2. Table 4 shows the average of $\log_{10} BF_{1N}$, $\log_{10} BF_{2N}$ and $\log_{10} BF_{AN}$ obtained from 1000 simulation replicates. Results here clearly demonstrate the merits of the proposed BMA-based approach. Additional simulations assuming a bigger effect ($EV = 0.05$) show that the averages of $\log_{10} BF_{1N}$, $\log_{10} BF_{2N}$ and $\log_{10} BF_{AN}$ are, respectively, 22.35, 2.29 and 21.65, if the true generating model is M_1. Even if the frequencies are not extreme, say $p_m = p_f = 0.3$ as in the application study, the averaged BMA-based quantity is clearly more robust as shown in Table 4, where the BMA-based $\log_{10} BF_{AN} = 1.755$, though not as high as $\log_{10} BF_{1N} = 1.942$ using the ideal (unknown) true model M_1, is clearly a substantial improvement over $\log_{10} BF_{2N} = 1.062$ using the incorrect model M_2.

When the allele frequency is on the boundary, we have commented that the resulting HPD intervals can be quite wide as seen in the application above e.g.

$rs12689325$ with MAF of 1.3%, the second ranked SNP in Figure 4; ranked 331 by the minimal p-value approach. Among the 14220 X-chromosome SNPs analyzed in Section 4, 829 SNPs have MAF less than 1%. In that case, there is little variation in the genotype variable thus limited information available for inference. The top ranked SNPs thus were chosen from the remaining 13391 SNPs with MAF greater than 1%. In recent years, joint analyses of multiple rare (or common) variants (also known as the gene-based analyses) have received much attention but only for autosome SNPs (Derkach *et al.*, 2014). Extension to X-chromosome SNPs remain an open question. Similarly, additional investigations are needed for X-chromosome SNPs in the areas of family-based association studies (Thornton *et al.*, 2012), direct interaction studies (Cordell, 2009), as well as indirect interaction studies via scale-test for variance heterogeneity (Soave & Sun, 2016).

In Table 1, allele D is assumed to be the risk allele with frequency ranging from 0 to 1, i.e. not necessary the minor allele. In practice as in our application, the minor allele is often assumed to be the risk allele based on the known genetic aetiology for complex traits. For autosome SNPs, it is well known that coding D or d as the reference allele leads to identical inference with $\beta_D = -\beta_d$. However, this is no longer true for analyzing X-chromosome SNPs under the no XCI M_2 model assumption; inference is identical under the XCI M_1 model; this was pointed out by (Wang *et al.*, 2014) in their frequentist's approach. To see the difference empirically in our Bayesian setting, we revisit the CF data as described in Section 4 and reanalyze SNP $rs3788766$ as a proof of principle. Specifically, we first assume the minor allele D as the reference allele under the XCI and no XCI assumptions, coded respectively as M_1-D and M_2-D. We then assume d as the reference allele and consider the corresponding M_1-d and M_2-d models. Table 5 shows the Bayes factor BF_{kN} comparing each model with the null model.

It is clear that the XCI M_1 model is robust to the choice of the underlying reference allele, i.e. M_1-D and M_1-d lead to identical association inference, but this is not the case for M_2-D and M_2-d under the assumption of no XCI. In hindsight this somewhat surprising results can be intuitively explained by the fact that under M_1, regardless of the choice of the reference allele, female dd and male d genotypes belong to one group, DD and D belong to another group and Dd itself is a group, i.e. $(\{dd, d\}, dD, \{DD, D\})$. Under M_2 the three groups are $(\{dd, d\}, \{dD, D\}, DD)$ when D is the reference allele in contrast of $(dd, \{dD, d\}, \{DD, D\})$ when d is the reference allele, thus resulting in different association quantities. However, we also note that in practice when allele frequencies are not close to the boundary as in this case (MAF = 0.388), the empirical difference between M_2-D and M_2-d is not significant; we provide additional application results in the Supplementary Materials. Nevertheless, it is worth noting that the choice of reference allele is yet another analytical detail that sets X-chromosome apart from the rest of the genome.

Acknowledgements

The authors would like to thank Dr. Lisa J. Strug for providing the cystic fibrosis application data, and Prof. Mike Evans for suggestions that have improved the presentation of the paper. This research is funded by the Natural Sciences and Engineering Research Council of Canada (NSERC) to RVC and LS, and the Canadian Institutes of Health Research (CIHR) to LS.

References

Choi, H. M., & Hobert, J. P. 2013. The Polya-Gamma Gibbs sampler for Bayesian logistic regression is uniformly ergodic. *Electronic Journal of Statistics*, **7**, 2054–2064.

Clayton, D. G. 2008. Testing for association on the X chromosome. *Biostatistics*, **9**, 593–600.

Clayton, D. G. 2009. Sex chromosomes and genetic association studies. *Genome Medicine*, **1**, 110.

Cordell, H. J. 2009. Detecting gene–gene interactions that underlie human diseases. *Nature Reviews Genetics*, **10**, 392–404.

Craiu, R. V., & Sun, L. 2014. *Bayesian methods in Fisher's statistical genetics world. In Statistics in Action: A Canadian Perspective.*

Derkach, A., Lawless, J. F., & Sun, L. 2014. Pooled association tests for rare genetic variants: a review and some new results. *Statistical Science*, **29**(2), 302–321.

Draper, David. 1995. Assessment and propagation of model uncertainty. *J. R. Stat. Soc. Ser. B Stat. Methodol.*, **57**(1), 45–97.

Gelman, A., & Meng, X. L. 1998. Simulating normalizing constants: from importance sampling to bridge sampling to path sampling. *Statistical Science*, **13**(2), 163–185.

Gendrel, A. V., & Heard, E. 2011. Fifty years of X-inactivation research. *Development*, **138**, 5049–5055.

Heid, I. M., Jackson, A. U., Randall, J. C., Winkler, T. W., Qi, L., & et al. 2010. Meta-analysis identifies 13 new loci associated with waist-hip ratio and reveals sexual dimorphism in the genetic basis of fat distribution. *Nat Genet*, **42**, 949–960.

Hickey, P. F., & Bahlo, M. 2011. X chromosome association testing in genome wide association studies. *Genet Epidemiol*, **35**, 664–670.

Hill, W. G., Goddard, M. E., & Visscher, P. M. 2008. Data and theory point to mainly additive genetic variance for complex traits. *PLOS Genet*, **4**(2), e1000008.

Hoeting, J.A., Madigan, D., Raftery, A.E., & Volinsky, C.T. 1999. Bayesian Model Averaging: A Tutorial. *Statistical Science*, **14**(4), 382–401.

Kass, R.E., & Raftery, A.E. 1995. Bayes factors. *Journal of the American Statistical Association*, **90**(430), 773–795.

Konig, I. R., Loley, C., Erdmann, J., & Ziegler, A. 2014. How to include chromosome X in your genome-wide association study. *Genet Epidemiol*, **38**, 97–103.

Lee, D., Bigdeli, T. B., Riley, B. P., Fanous, A. H., & Bacanu, S. A. 2013. DIST: direct imputation of summary statistics for unmeasured SNPs. *Bioinformatics*, **29**(22), 2925–2927.

Loley, C., Ziegler, A., & Konig, I. R. 2011. Association tests for X-chromosomal markers – a comparison of different test statistics. *Human Heredity*, **71**, 23–36.

Meng, X. L., & Wong, W. H. 1996. Simulating ratios of normalizing constants via a simple identity: a theoretical exploration. *Statistica Sinica*, **6**, 831–860.

Pasaniuc, B., Zaitlen, N., Shi, H., Bhatia, G., Gusev, A., & et al. 2014. Fast and accurate imputation of summary statistics enhances evidence of functional enrichment. *Bioinformatics*, **30**(20), 2906–2914.

Polson, N. G., Scott, J. G., & Windle, J. 2013. Bayesian inference for logistic models using Polya-Gamma latent variables. *Journal of the American Statistical Association*, **108**, 1339–1349.

Sasieni, P. D. 1997. From genotypes to genes: doubling the sample size. *Biometrics*, **53**(4), 1253–1261.

Soave, D., & Sun, L. 2016. A Generalized Levene's Scale Test for Variance Heterogeneity in the Presence of Sample Correlation and Group Uncertainty. *arXiv:1605.05715*.

Stephens, M., & Balding, D. J. 2009. Bayesian statistical methods for genetic association studies. *Nature Reviews Genetics*, **10**, 681–690.

Sun, L., Rommens, J. M., Corvol, H., Li, W., Li, X., & et al. 2012. Multiple apical plasma membrane constituents are associated with susceptibility to meconium ileus in individuals with cystic fibrosis. *Nature Genetics*, **44**(5), 562–569.

Teslovich, T. M., Musumuru, K., Smith, A. V., Edmondson, A.C., Stylianou, I. M., & et al. 2010. Biological, clinical and population relevance of 95 loci for blood lipids. *Nature*, **466**, 707–713.

Thornton, T., Zhang, Q., Cai, X. C., Ober, C., & McPeek, M. S. 2012. XM: Association Testing on the X-Chromosome in Case-Control Samples With Related Individuals. *Genet Epidemiol*, **36**, 438–450.

Wang, J., Yu, R., & Shete, S. 2014. X-chromosome genetic association test accounting for X-inactivation, skewed X-Inactivation, and escape from X-inactivation. *Genet Epidemiol*, **38**, 483–493.

Welter, D., MacArthur, J., Morales, J., Burdett, T., Hall, P., & et al. 2014. The NHGRI GWAS Catalog, a curated resource of SNP-trait associations. *Nucleic Acids Research*, **42 (Database issue)**, D1001–D1006.

Wise, A. L., Gyi, L., & Manolio, T. A. 2013. eXclusion: toward integrating the X chromosome in genome-wide association analyses. *Am J Hum Genet*, **92**, 643–647.

Wright, J. H. 2008. Bayesian model averaging and exchange rate forecasts. *Journal of Econometrics*, **146**, 329–341.

Zellner, A. 1986. On assessing prior distributions and Bayesian regression analysis with g-prior distributions. *Pages 233–243 of:* Goel, P. K., & Zellner, A. (eds), *Bayesian Inference and Decision Techniques: Essays in Honour of Bruno de Finetti.* North-Holland, Amsterdam.

Zheng, G., Joo, J., Zhang, C., & Geller, N. L. 2007. Testing association for

markers on the X chromosome. *Genet Epidemiol*, **31**, 834–843.

TABLE 1
Genotype coding under the X-chromosome inactivation (XCI, M_1) and no X-chromosome inactivation (no XCI, M_2) assumptions

		Female			Male	
Model	Coding	*dd*	*dD*	*DD*	*d*	*D*
M_1: XCI	G_1	0	0.5	1	0	1
M_2: no XCI	G_2	0	1	2	0	1

TABLE 2
Summary of frequentist analysis of four top ranked SNPs, selected from analyzing association evidence between 14220 X-chromosome SNPs and meconium ileus in 3199 Cystic Fibrosis patients. MAF is the pooled estimate of the frequency of the minor allele (frequencies do not differ between males and females), log odds ratio estimates under the XCI M_1 and no XCI M_2 assumptions, and their corresponding p-values and the (adjusted) p-value of the minimal p-value or the maximal Z value.

		Log Odds Ratios		P-values		
SNPs	MAF	M_1	M_2	M_1	M_2	Z_{max}
$rs3788766$	0.388	0.798	0.484	8.50e-12	2.20e-09	1.61e-11
$rs5905283$	0.487	0.586	0.326	4.79e-08	9.64e-06	8.88e-08
$rs12839137$	0.237	0.611	0.360	7.55e-06	5.44e-04	1.25e-05
$rs5905284$	0.249	0.592	0.358	8.61e-06	1.21e-04	1.43e-05

TABLE 3
Summary of Bayesian analysis of 15 top ranked SNPs, selected from analyzing association evidence between 14220 X-chromosome SNPs and meconium ileus in 3199 Cystic Fibrosis patients. SNP are ordered based on their lower bounds of the BMA-average HPD intervals for β.

		HPD intervals		Bayes factors	
SNPs	MAF	Lower	Upper	BF_{12}	BF_{AN}
$rs3788766$	0.388	0.572	1.033	2.71e+02	1.49e+09
$rs12689325$	0.013	0.405	3.118	3.77e -01	3.28e+00
$rs5905283$	0.487	0.379	0.784	2.02e+02	8.71e+04
$rs12845594$	0.047	0.344	1.700	7.23e+00	8.61e+00
$rs12839137$	0.237	0.307	0.884	2.25e+01	1.34e+03
$rs5905284$	0.249	0.302	0.830	1.83e+01	1.08e+03
$rs579854$	0.136	0.266	0.932	1.88e+00	4.83e+01
$rs5955417$	0.030	0.260	2.130	3.28e+00	5.30e+00
$rs12720074$	0.100	0.237	0.943	5.33e -01	5.49e+01
$rs1921965$	0.091	0.228	0.893	1.34e+00	2.81e+01
$rs6623182$	0.036	0.217	1.216	2.89e+00	9.08e+00
$rs3027514$	0.015	0.209	1.496	8.34e -01	1.34e+00
$rs17338514$	0.099	0.201	0.821	1.19e+00	2.09e+01
$rs11797786$	0.068	0.191	0.947	4.68e+00	4.47e+00
$rs1921967$	0.122	0.190	0.756	7.50e -01	2.52e+01

TABLE 4
Summary of the average of log_{10} (Bayes factors) based on 1000 independent simulation replicates. Allele frequency of D is 0.95 or 0.3 for both male and female, sample size is 1000, EV = 0.01, and data are simulated from the XCI M_1 model or no XCI M_2 model. BF_{1N}, BF_{2N} and BF_{AN} are the Bayes factors of M_1 vs. the null M_N model, the no XCI M_2 vs. M_N, and the BMA-based model vs. M_N.

(p_m, p_f)	True Model	$\log_{10} BF_{1N}$	$\log_{10} BF_{2N}$	$\log_{10} BF_{AN}$
$(0.95, 0.95)$	M_1	2.066	-1.850	1.541
$(0.95, 0.95)$	M_2	-1.969	1.854	1.309
$(0.30, 0.30)$	M_1	1.942	1.062	1.755
$(0.30, 0.30)$	M_2	1.073	1.983	1.796

TABLE 5
Bayes factors of comparing models assuming different risk reference allele (D or d) and genotype codings (XCI M_1 or no XCI M_2) of SNP rs3788766 with the null model, based on the Cystic Fibrosis application data.

	Female			Male		
Model	dd	dD	DD	d	D	BF_{kN}
M_1-D	0	0.5	1	0	1	2.97e+09
M_1-d	1	0.5	0	1	0	2.97e+09
M_2-D	0	1	2	0	1	8.21e+06
M_2-d	2	1	0	1	0	1.74e+06

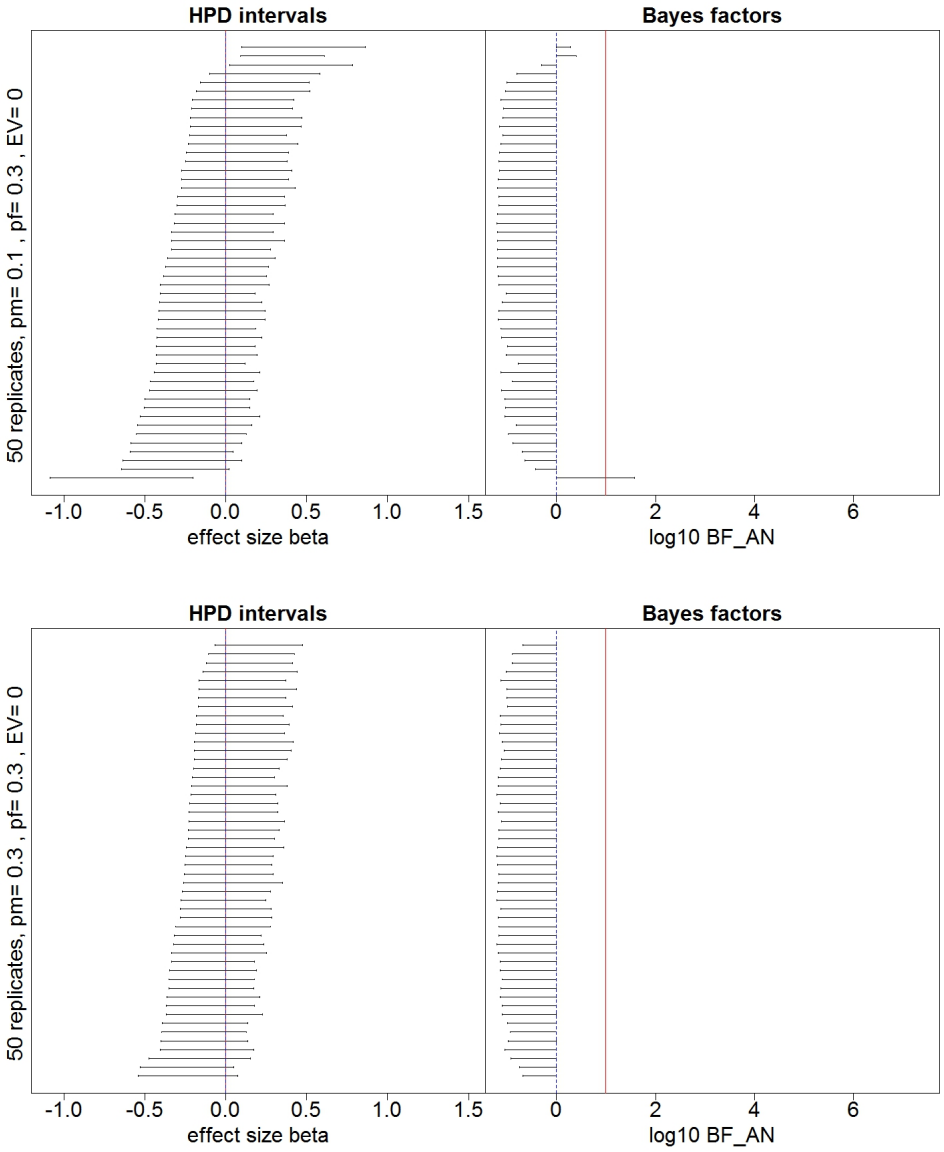


FIG 1. *BMA-based HPD intervals for β (left panel) and corresponding $log_{10}(BF_{AN})$ (right panel) for 50 replicates simulated based on null M_N* **logistic model**. *Intervals are sorted by their lower bounds. Male and female allele frequencies are* $(0.1, 0.3)$ *(top panel) and* $(0.3, 0.3)$ *(bottom panel). In the left panel, the blue dashed line and red solid line overlap at the null value of $\beta = 0$. In the right panel, the blue dashed line and red sold line mark, respectively, $log_{10}(BF_{AN}) = 0$ and $= 1$.*

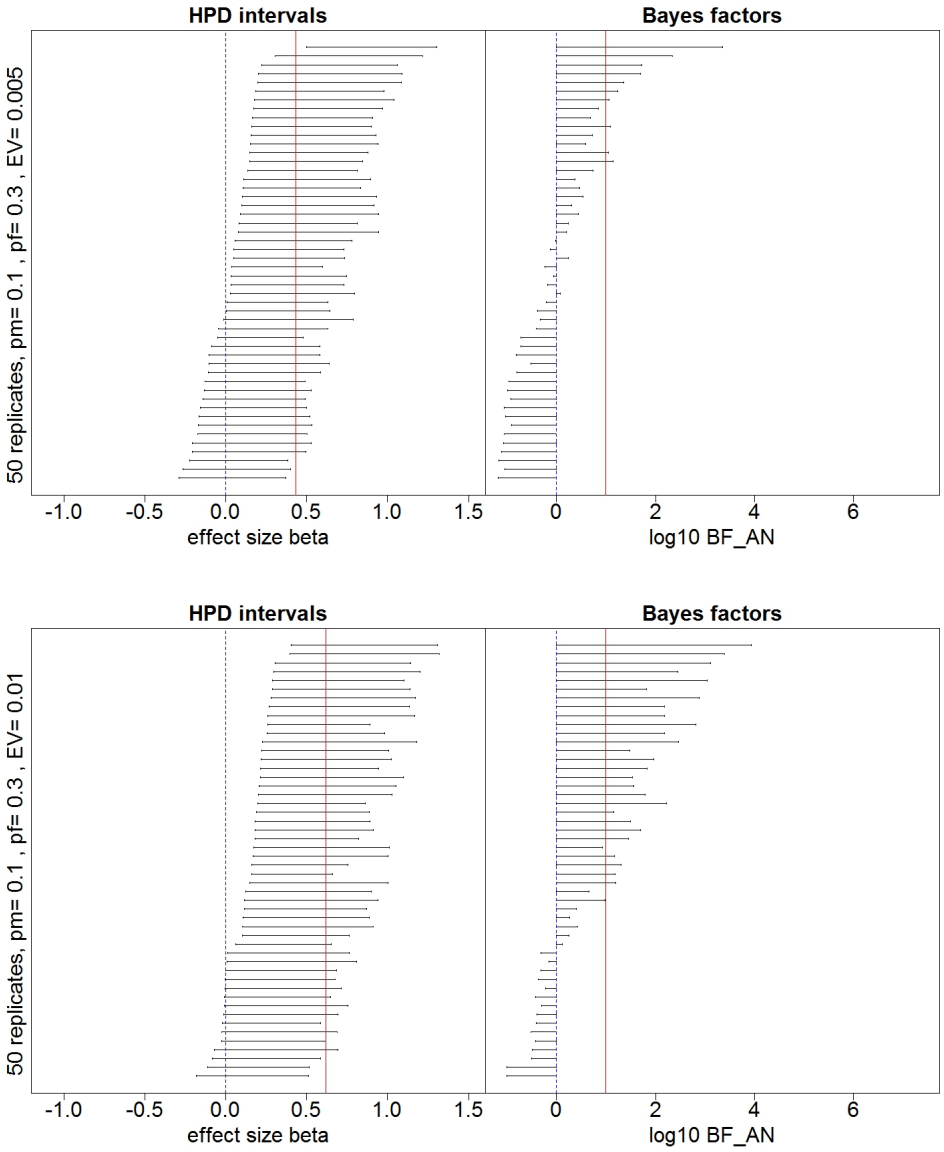


FIG 2. *BMA-based HPD intervals for β (left panel) and corresponding $log_{10}(BF_{AN})$ (right panel) for 50 replicates simulated based on XCI M_1* **logistic model**. *Intervals are sorted by their lower bounds. Male and female allele frequencies are* $(0.1, 0.3)$. *In the left panel, the blue dashed line marks the null value of* $\beta = 0$, *and the red solid line marks the true value of* β, *determined so that* $EV = 0.005$ *(top panel) and* $EV = 0.01$ *(bottom panel). In the right panel, the blue dashed line and red sold line mark, respectively,* $log_{10}(BF_{AN}) = 0$ *and* $= 1$.

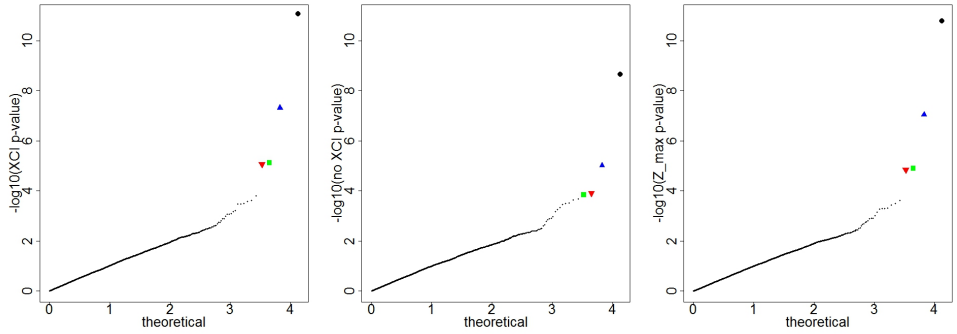


FIG 3. *QQplots of $-log_{10}$ p-values of analyzing association evidence between 14220 X-chromosome SNPs and meconium ileus in 3199 Cystic Fibrosis patients, under the XCI M_1 assumption (left), the no-XCI M_2 assumption (middle) and using Z_{max} (right). Black circle • for rs3788766, blue up-pointing triangle ▲ for rs5905283, green square ■ for rs12839137 and red down-pointing triangle ▼ for rs5905284.*

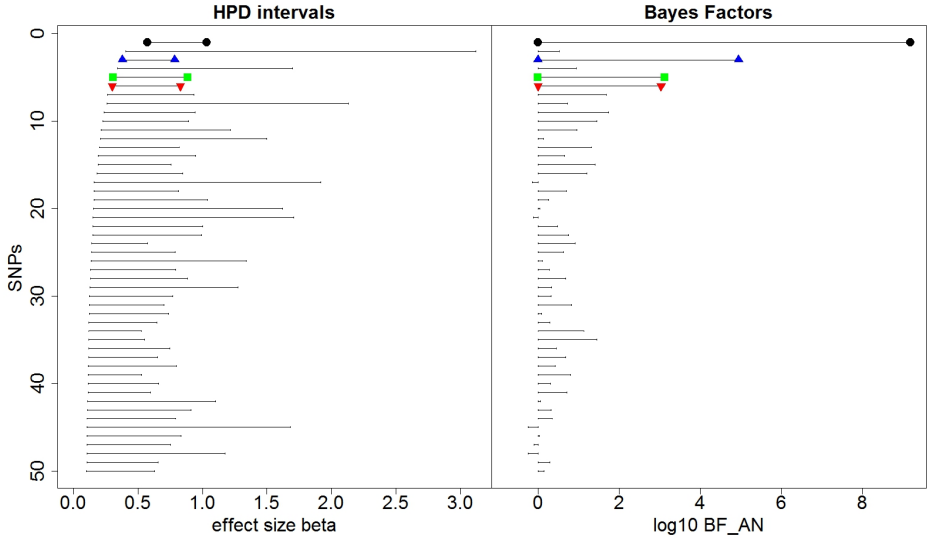


FIG 4. *BMA-based HPD intervals for β and corresponding $log(BF_{AN})$ for 50 top ranked SNPs, selected from analyzing association evidence between 14220 X-chromosome SNPs and meconium ileus in 3199 Cystic Fibrosis patients. SNP are ordered based on their lower bounds of the HPD intervals. The four top SNPs identified by p-values are marked here using the same symbol: black circle • for rs3788766, blue up-pointing triangle ▲ for rs5905283, green square ■ for rs12839137 and red down-pointing triangle ▼ for rs5905284.*